

Scott T. Shipley¹, Ira A. Graffman², Robert E. Saffle³, and Joseph Facundo⁴
 Environmental Resource Technologies, National Weather Service, Mitretek Systems,
 and George Mason University
 Silver Spring, Maryland

1. INTRODUCTION

Desktop Geographic Information System (GIS) tools have been developed and tested for operational applications in weather radar siting and radar beam propagation analysis. Radar characteristics and atmospheric propagation parameters are input variables. Radar beam blockage is estimated using digital elevation models, plus additional information on vegetation and manmade obstacles. Our technique compares favorably with the original NEXRAD site surveys conducted by Stanford Research Institute (SRI), and duplicates independent results provided by the NEXRAD Radar Operations Center (ROC). Verification is performed using Level 2 data. Results include triangulation to radar location, estimation of radar sampling voids due to terrain occultation, and verification of radar refraction models.

The GIS technique for radar siting has been described in this forum several times (Saffle et al., 2003; Shipley et al., 2005a) and has enjoyed continued support by the Office of Science and Technology, Systems Engineering Center. Latest developments in 2005 include a streamlining of the Nex2Shp utility to support siting analysis with a minimum number of independent input parameters, resulting in a new release of Nex2Shp (version 8c) to GNU license with open source (Shipley, 2005b). The overall GIS analysis procedure under ArcGIS™ 9.1 (ESRI, 2005) is migrating to Model Builder (an application bundled with ArcGIS) to support the development and use of a set of tools or “toolbox” for radar data processing. Details of the Nex2Shp utility and Model Builder analysis approach are provided in section 2.

The results of the GIS-based procedure are compared with the original results provided by surveys conducted by SRI (Leone et al., 1989), which are also the current NWS operational

¹Corresponding author – Scott T. Shipley, Environmental Resource Technologies, Inc., Jessup, Maryland. Please contact c/o Department of Geography, George Mason University, Fairfax, Virginia 22030, Mail Stop 1E2, sshipley@gmu.edu.

²Ira A. Graffman, National Weather Service, Silver Spring, MD, Ira.Graffman@noaa.gov.

³Robert E. Saffle, Mitretek Systems, Silver Spring, MD, Robert.Saffle@noaa.gov.

⁴Joseph Facundo, National Weather Service, Silver Spring, MD, Joseph.Facundo@noaa.gov.

standard. In addition, independent verification of occultation patterns can be obtained using Level II data. Samples of comparison to these standards are discussed in Section 3.

2. OVERVIEW OF THE PROCEDURE

The technical approach estimates radar beam occultation on a “cell by cell” basis, following an idealized radar energy pulse along a radial at each azimuthal angle α , as the centroid of radio energy rises (or falls) with respect to the Earth Geoid starting at beam elevation angle ϵ . This technique has been outlined by Saffle (2003), then with the National Weather Service (NWS) Office of Science and Technology, and is similar to the original NEXRAD occultation techniques employed by Leone et al. (1989). The current approach has been demonstrated using the Commercial Off-The-Shelf (COTS) ArcView™ GIS by ESRI. The NWS maintains a version of this technique in Avenue™ for application with ArcView 3.x, since that capability can be operated across several operating systems including Windows™, UNIX and Linux. The GIS-based technique requires the Spatial Analyst™ and 3D Analyst™ extensions.

Radar cell centroid locations and height above the Earth Geoid are calculated using a Visual Basic (VBa) utility, Nex2Shp version 8c or later, which is provided freely to public domain for Windows (Shipley, 2005b). This utility produces point Shapefiles™ for input to the occultation analysis procedure. The NEX2SHP utility also decodes Level 3 NEXRAD product #19 (Radar Reflectivity), and can produce GIS-compatible polygon or point features as a function of {lon, lat, z} from NEXRAD radar measurements. Version 8c of the NEX2SHP utility updates the height approximation released in version 2, with an improved range-height equation introduced by Saffle (2003). The version 8c utility has also been generalized to create radar beam test patterns for additional radars including the FAA TDWR.

The sequence of processing steps lends itself to representation in Model Builder, as shown in Figure 1. After the input parameters are finalized in a text file, the Nex2Shp utility creates a point shapefile (**Point Shape 1**) which is used to create a GRID surface (Radar Surface) useful for 3D displays in viewers such as ArcScene™. The Nex2Shp product is combined with a digital elevation model (DEM) to append elevation of the

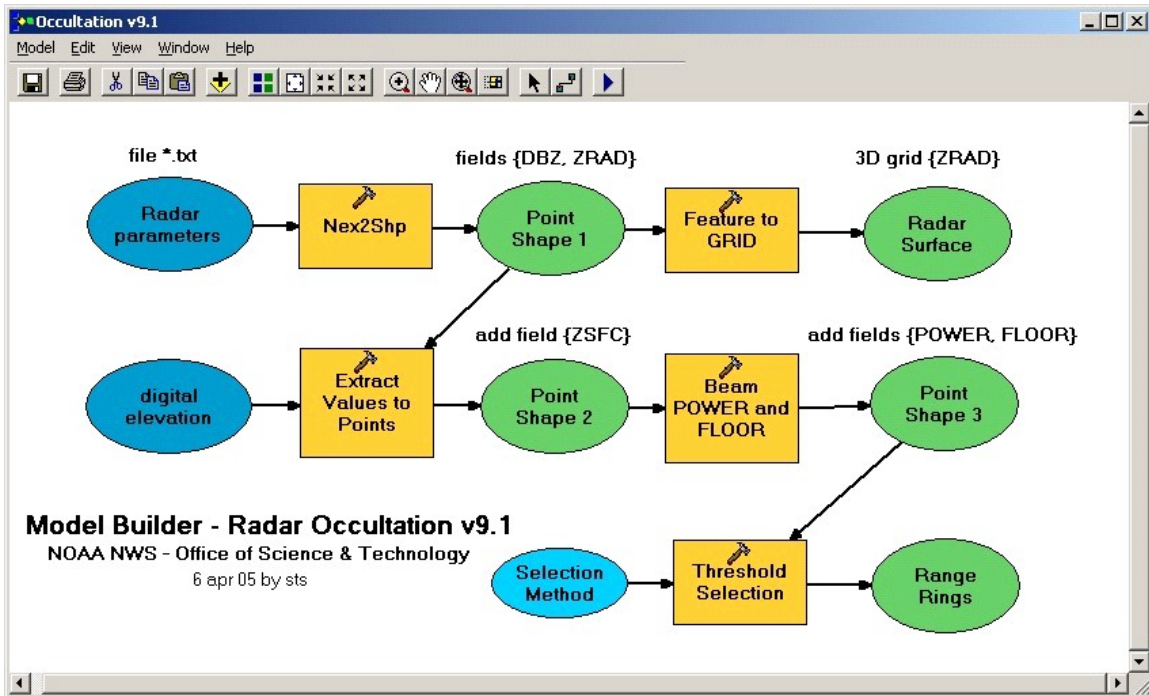


Figure 1 – Model Builder diagram for the automatic creation of range rings from a radar parameter file without additional user interaction. The user must also specify the selection method, which is typically set to (Power < 50%) OR (Height > 10 kft ARL). The term ARL is defined in Figure 2. The Radar Occultation model can also be run as a tool, or called from a script.

surface as the field [Zsfc] in meters msl and output as **Point Shape 2**. Each radar cell is then processed record by record to determine both a beam power reduction factor {0% ≤ Power ≤ 100%}, and the [Floor] in meters msl, which is interpreted as the minimum height for detection of precipitation (**Point Shape 3**). A final threshold method selects one point along each radial where the beam reaches a detectability threshold (programmable), and these points are converted into “range rings” (polyline and polygon).

2.1 Nex2Shp Utility

When the input data file is a text file with extension *.txt, the NEX2SHP utility attempts to interpret the contents as named parameters. If valid, these parameters are then used to create a theoretical radar feature dataset, currently in the Shapefile format. The contents of the text file are interpreted as shown in Table 1. If omitted, the default values for optional parameters are assumed to describe a NEXRAD system as shown in Table 1. A Shapefile consists of, at a minimum, three files with identical filenames: *.shp providing the shape description, *.dbf providing the tabular (relational) data records for each shape, and *.shx providing an index between the spatial and relational contents. If only two parameters are supplied, then the utility will create a point shapefile and will not include lon/lat fields in the table. NEX2SHP does not

directly create a geodatabase. The utility also supports a command line execution mode, namely:

```
nex2shp infile, outfile, Point/Poly, IncLonLat (1)
```

where:

infile	input file as “path/filename.ext”
outfile	output file as “path/filename”
Point/Poly	string = “point” or “poly”
IncLonLat	string = “yes” if desired in table

Table 1 – Input parameters for NEX2SHP 8c

lat	<u>39.00</u>	* radar latitude [decimal degrees]
lon	<u>-100.05</u>	* radar longitude [decimal degrees]
zmsl	<u>1500</u>	* local ground level at radar base [m MSL]
elevangle	0.5	* elevation angle [decimal degrees]
towerheight	30	* height of antenna above ground [m AGL]
numradials	360	number of azimuthal samples per scan
numrangebins	230	number of range bins per azimuth
rangebinlength	1.0	length of each range bin [km]
verticalbeamwidth	1.0	vertical beam angular width [decimal degrees]

* indicates required parameter

2.2 Vertical Beam Height vs. Range

The height of the radar beam centroid for WSR-88D (NEXRAD) volume coverage patterns is calculated following Saffle et al. (2003), namely:

$$h(r, \varepsilon) \approx (r^2 \cos^2 \varepsilon / 2aR_E) + r \sin \varepsilon \quad (2)$$

where:

h	height of beam centroid ARL (Above local Radar Level)
r	horizontal range
ε	radar elevation angle
a	Effective Earth Radius factor
R_E	Radius of the Earth.

This formula has been tested for negative beam elevation angles ($\varepsilon < 0$), and has been shown to be appropriate in the domain $\{-1^\circ < \varepsilon < +20^\circ\}$. For direct line-of-sight (no ducting), it can also be shown to a first approximation that :

$$h(r, \varepsilon) \approx (r^2 / 2R_E) + r \sin \varepsilon \quad (3)$$

Using the small angle approximation for ε and neglecting the ε^2 term, then Eq. (2) can be inverted to yield:

$$\varepsilon \approx (h/r) - (r/2aR_E) \quad (4)$$

Eq. (4) can now be used to estimate the so-called "SRI range" for NEXRAD, where a beam just clearing an obstacle of height h at range r will reach $h = 10$ kft at the same elevation angle at $r = 230$ km. What is missing is a relationship between

range r and Great Circle distance S . Nex2Shp has used the following approximation:

$$S \approx r \cos \varepsilon (1 - (h/R_E)) \quad (5)$$

2.3 Terrain Database Interaction

The NEX2SHP version 8c utility estimates radar beam centroid location in x (longitude), y (latitude) and z (height msl). The GIS technique uses this information to sample a Digital Elevation Model (DEM) at the location $\{\text{lon}, \text{lat}\}$ of each centroid, and adds fields for terrain height $[Z_{\text{sfc}}]$ to derive the relative height of the beam centroid above local terrain. The figures provided in this paper use the 30 arcsec DEM provided with AWIPS, see Graffman (2004), although finer resolution DEMs can be inserted. The current technique approximates beam occultation by sampling at the beam centroid, so higher resolution DEMs are not currently justified except at close ranges.

2.4 Estimating Obstruction along Radials

The NEXRAD beam centroid table is manipulated as a point Shapefile, and is organized by range and radial running in range from 1...230 km, then by radial from 0...359 degrees azimuth. Additional fields $[\text{Power}]$ and $[\text{Floor}]$ are added to record theoretical obstruction in percent and the lowest height of the unobstructed beam. Occultation is accumulated along each radial in the field $[\text{Power}]$, which is estimated for each cell along a radial, but impacts $[\text{Power}]$ only if it is a smaller value, since $[\text{Power}]$ can only go down when interacting with a lossy medium.

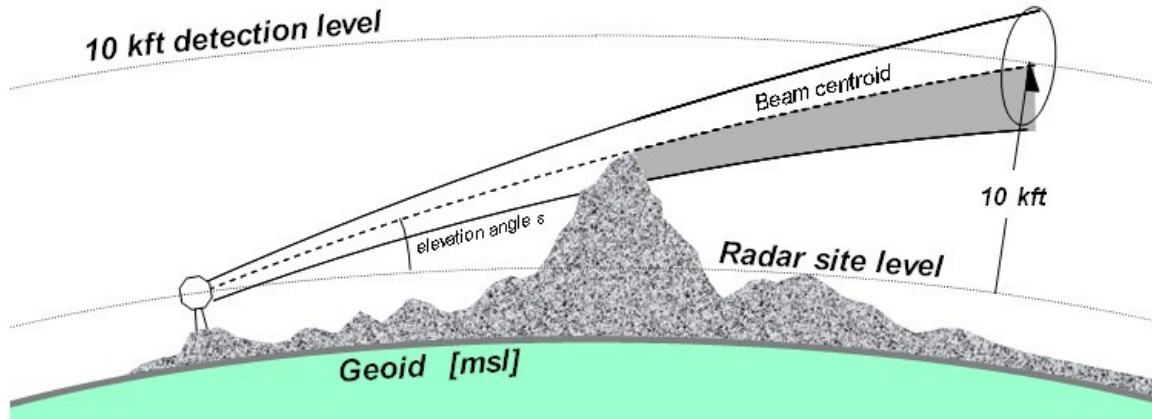


Figure 2 – Theoretical WSR-88D beam propagation path for initial beam elevation angle ε . The radar beam power distribution is assumed to be symmetric about the beam centroid. The lowest detectable height is defined by the bottom of the beam, which in this paper is called the "Floor". When the occultation criterion is set to $\text{Power} < 50\%$, then the Floor is defined by the beam centroid after that centroid grazes an obstacle. The SRI method (Leone et al., 1989) defines the maximum detectable range when the lowest possible beam centroid reaches 10 kft ARL (Above Radar Level), and radar beam elevation angles are presumed to vary continuously. The vertical scale is greatly exaggerated.

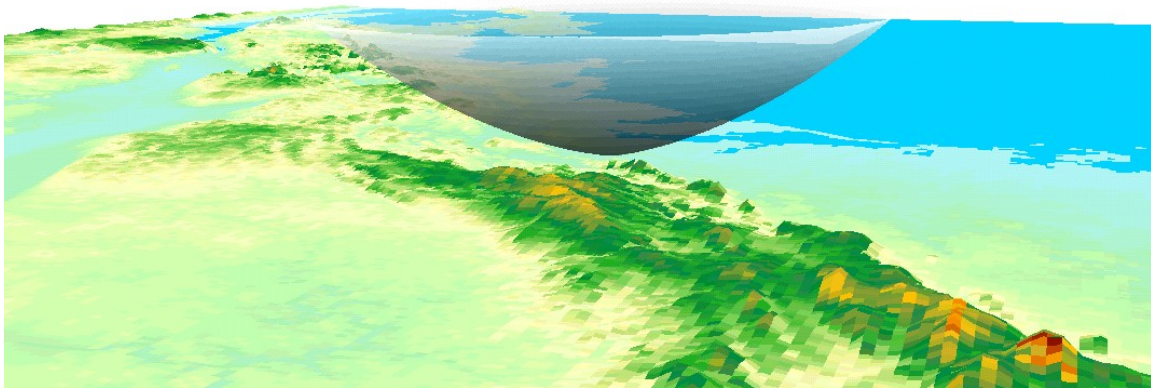


Figure 3a – Superposition of the theoretical beam pattern generated by the NEX2SHP utility and local terrain for KLWX, the WSR-88D located at Sterling, VA, at a beam elevation angle of 0.5 degrees. This 3D view was created using ESRI ArcScene™ (provided with the 3D Analyst extension), looking towards the NE along the Appalachian Mountains. The surface indicates height of the radar beam centroid above mean sea level.

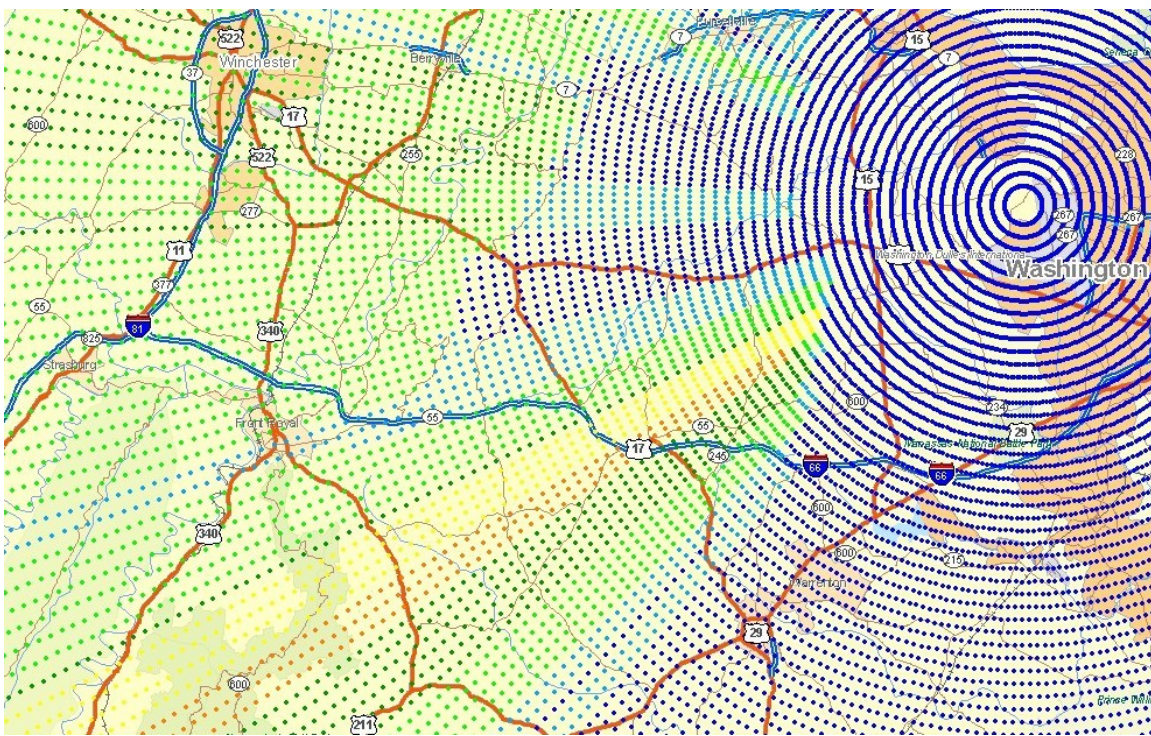


Figure 3b – NEXRAD centroids for each range cell as points on the surface shown in Figure 3a, for KLWX at a beam elevation angle of 0.5 degrees, overlaid onto SteetMap USA™. A ten-level color scheme is used to identify fractional Power loss due to occultation, with red-yellow below 50% and green-blue above 50%. Significant occultation is calculated SouthWest of KLWX due to the nearby Bull Run Mountains, located just North of Interstate I66 and West of US Highway 15.



Figure 3c – Panoramic photo of NEXRAD at KLWX (just left of center) looking West along County Highway 606, at the junction with Route 28 in Sterling, VA. The Bull Run Mountains can be clearly seen to the SouthWest.

The current technique uses a simplifying assumption of a rectangular or “square” vertical distribution for beam energy. Therefore, $[Power]_i$ can be estimated at each point $[Zrad]_i$ along the radial using the height of the centroid above obstructions $[Zsfc]_i$, such that

$$[Power]_i = \frac{1}{2} + ([Zrad]_i - [Zsfc]_i) / b \quad (6)$$

for $0 < [Power]_i < 1$, and where b is vertical beamwidth in meters. The parameter $[Floor]$ is determined by $[Zsfc]$ when $[Power]_i < 1$, and must be propagated to longer ranges for the corresponding beam elevation angle ϵ_i as shown in Figure 2.

An example of this process for NEXRAD KLWX located in Sterling, VA, is shown in Figures 3. Figure 3a shows the beam centroid surface $[Zrad]$ corresponding to a beam elevation angle of 0.5 degrees (grid **Radar Surface** in Figure 1), located above $[Zsfc]$ (grid **digital elevation** in Figure 1). A map of the radar cell centroids with symbolization for $[Power]$ (**Point Shape 3** in Figure 1) is given in Figure 3b, showing significant occultation ($[Power] < 50\%$) at 0.5 degree beam elevation due to the nearby Bull Run Mountains. A panoramic image of the scene showing KLWX and the Bull Run Mountains is presented in Figure 3c.

2.5 Feature Extraction

The full set of centroids for KLWX at 0.5 degree beam elevation is shown in Figure 4. The point symbolization scheme is identified in the legend to the left of this figure. Each point has a table record or “attributes” providing the pertinent information for that point, as shown in Figure 5. The threshold method is now applied to “select” one point in each radial where the threshold criterion is satisfied. Our most common threshold is $[Power] < 50\%$, which defines that point where beam power is decreased

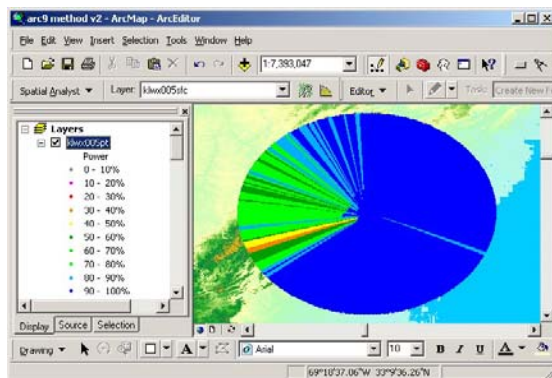


Figure 4 – “Point Shape 3” in Figure 1 for KLWX at a beam elevation angle of 0.5 degrees. The field $[Power]$ is symbolized with a color scheme from red (occulted) to blue (not occulted).

to the half-power level. If no points are found which meet the threshold criterion, then the last point must be selected, assuring that one point is selected for each and every radial. The resulting selection for KLWX at 0.5 degree beam elevation and for the criterion ($[Power] < 50\%$) is shown in Figure 6. The original SRI method uses an additional condition that $[Zsfc]$ does not exceed the local radar height by 10 kft. The selection corresponding to the original SRI method is shown in Figure 7.

FID	Shape	DBZ	ZRAD	ZSFC	Power	Floor
0	Point	1	126	85	1	117.274
1	Point	2	135	91	1	126.274
2	Point	3	144	67	1	135.274
3	Point	4	154	73	1	145.274
4	Point	5	163	73	1	154.274
5	Point	6	172	73	1	163.274
6	Point	7	182	73	1	173.274
7	Point	8	192	73	1	183.274
8	Point	9	202	73	1	193.274
9	Point	10	212	91	1	203.274
10	Point	11	222	61	1	213.274
11	Point	12	232	61	1	223.274
12	Point	13	243	73	1	234.274
13	Point	14	253	91	1	244.274
14	Point	15	264	91	1	255.274
15	Point	16	275	91	1	266.274
16	Point	17	286	85	1	277.274
17	Point	18	297	91	1	288.274
18	Point	19	308	91	1	299.274

Figure 5 – A small subset of the attributes for the 82,800 point collection of “Point Shape 3” in Figure 4. When generating radar test patterns, Nex2Shp uses the field $[Dbz]$ to show range bin number (1...230 for NEXRAD) and a special point is added with $[Dbz] = 0$ for the radar site itself. Nex2Shp also calculates $[Zrad]$ as the height of the radar beam centroid in meters MSL. The tool “Extract Values to Points” extracts $[Zsfc]$ from a digital elevation model, and tool “Beam Power and Floor” creates and calculates just what it says.

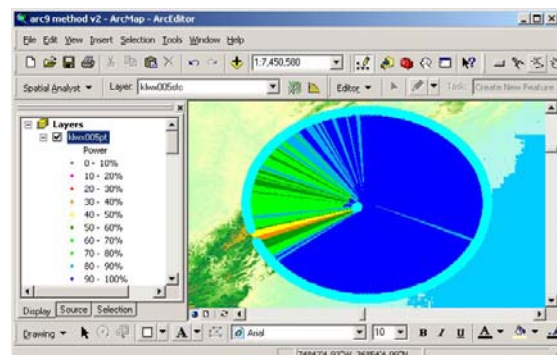


Figure 6 – The tool “Threshold Selection” selects one point along each radial which is the first to meet selection criteria, and the selected points are indicated by the user-defined highlight color (cyan in this example). The selection method shown here is ($[Power] < 50\%$) or ($[Dbz] = 230$). For NEXRAD, there are 360 radials so 360 points are selected.

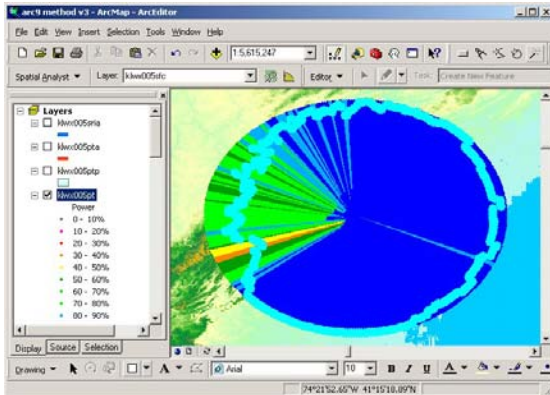


Figure 7 – NEXRAD KEMX with the threshold selection method set to “SRI”, which is lowest achievable beam elevation angle (a continuous variable) and beam height > 10 kft ARL. Lowest achievable elevation angle is that angle which just clears all obstacles along the radar beam path.

3. Comparison with Standards

The original SRI range ring for the KLWX site survey is compared to the GIS-method range ring for SRI threshold criteria in Figure 8. The authors currently suspect that the minor difference in occultation range results for the Bull Run Mountains is related to beam propagation assumptions, since the SRI site survey appears to have used obstruction sitings obtained by optical propagation. This is an area that needs further resolution. For practical siting purposes, these results are identical.

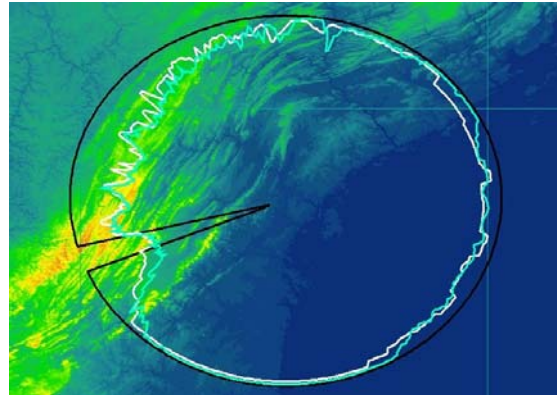


Figure 8 – Comparison of the GIS-based method (white range ring) with the original SRI range ring (black), which clearly shows occultation associated with the Bull Run Mountains SouthWest of KLWX. The two methods for “SRI range ring” are in excellent agreement.

The goal of this exercise is to validate and/or reproduce the original NEXRAD site surveys commissioned by the NWS and executed by Stanford Research Institute (Leone et al., 1989). These SRI results are available from the NWS as polyline Shapefiles. The original site survey not only accounts for occultation by terrain and manmade obstructions, but also estimates the radar coverage volume for detectable regions located below 10 kft (Leone et al., 1989, state that the limiting altitude is 6 kft). The exact definition of the sample volume is being precisely defined, but it is generally thought that radar coverage is available when beam energy is above 50% (occultation) and the sample volume is located within 10 kft of the surface (local terrain elevation). The SRI results are generally reproduced when the sample volume is truncated at 10 kft ARL.

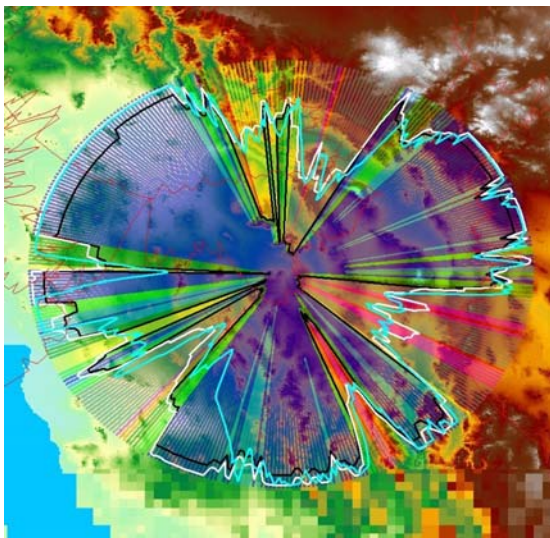


Figure 9 – Comparison to the original SRI NEXRAD site survey coverage pattern (cyan) for KEMX “range rings” (Tucson, AZ at Empire Mountain). The GIS-based method to reproduce SRI (white) does not compare in every detail. Also shown for reference is the theoretical calculation of the 50% Power range ring for one azimuthal scan at a beam elevation angle of 0.5 degrees (black).

A detailed comparison of these two methods is provided in Figure 9 for NEXRAD KEMX near Tucson, AZ. The SRI standard range rings are similar but there are significant differences, particularly to the SSW of KEMX. One key difference is a systematic shift of the occultation patterns, as though the radar positions are slightly different. As shown in Figure 10, the occultation features in the range rings can be used to triangulate to an original radar location, especially when the occultation is produced by a relatively isolated terrain feature such as the Santa Rita Mountains (the grey-white terrain cells in Figure 10). KEMX location was provided as (-110.6303, +31.8936) in decimal degrees. The original SRI results appear to point to the highest terrain elevation for the Empire Mountains, which would be the expected location for a NEXRAD. The location

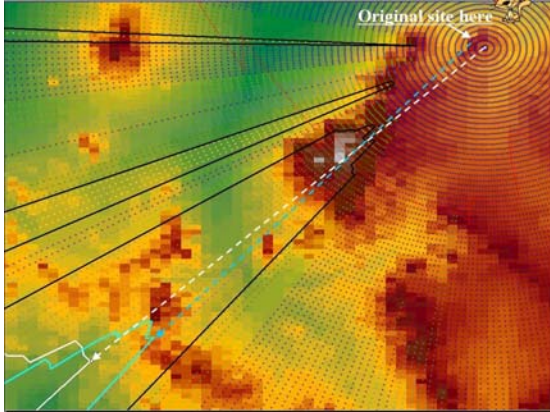


Figure 10 – Zooming in to the area SouthWest of KEMX (from Figure 9), the occultation patterns for the original SRI (cyan) and the GIS method (white) appear to have an angular offset. The radial for an occultation feature can be traced back to the radar site (dashed white line), showing it's association with high terrain (grey-white grid cells). The original SRI range ring traces this feature back to an adjacent DEM cell which has significantly higher elevation, and which would be the likely location for a NEXRAD site. We suggest that either the KEMX coordinates given are incorrect, or the original site surveyed by SRI was displaced 0.02 decimal degrees to the WNW of the current location of KEMX as provided by the NWS.

provided for KEMX appears to be 0.02 decimal degrees to the ESE of this point, which is also about 100 m lower in digital elevation. Such discrepancies can be avoided with today's technology, and clearly the NWS needs to produce a verified set of NEXRAD coordinates which provides the radar tower locations in line with the WGS 84 datum (the current US standard for interagency exchange of geographic information).

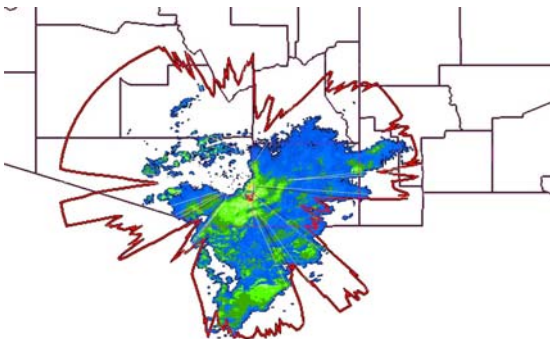


Figure 11 – An experimental verification of the “range rings” can be accomplished using NEXRAD Level II data. Shown in this figure is the summation of reflectivity for one scan cycle on 1 Jan 2004 at 0425 ut, using the lowest four elevation angles. We would not expect to see radar echoes external to the theoretical beam pattern.

Another method for range-ring verification is experimental, but is only available for existing NEXRAD installations. As shown in Figure 11, NEXRAD Level II data is obtained from NCDC (Ansari and Del Greco, 2005) for the four lowest beam elevation angles (0.44, 1.49, 2.42 and 3.38 degrees beam elevation). These data are superimposed to derive a sample of echoes in the region. If the occultation rings are correct, then there should be few precipitation echoes outside of the range rings. In Figure 11, there is a small area of echoes outside the range ring to the ESE of KEMX which appears only with the 1.49 degree beam elevation angle. These echoes are probably associated with precipitation higher than 10 kft ARL.

4. Recommendations for Improvement

A comparison to current standards for radar occultation patterns includes products generated by the NEXRAD Radar Operations Center (ROC), and original NEXRAD siting studies developed by Stanford Research Institute, all showing general agreement. Factors leading to variations among these approaches include:

- 1) Range-Height beam propagation – Significant at longer ranges, Effective Earth Radius coefficients for radar beam propagation vary among the approaches, typically 4/3 or 6/5.
- 2) Atmospheric ducting for non-standard atmospheres – The 4/3 and 6/5 Effective Earth Radius coefficients assume an ICAO Standard Atmosphere without temperature inversions in the lower troposphere.
- 3) Radar sample volume definition, primarily vertical beam power distribution – The current approach assumes that beam power is distributed uniformly with height across the *vertical beamwidth* (an input parameter).
- 4) Horizontal beam spread and DEM resolution – The current GIS application assumes that all radar energy is located at the centroid of the radar sample volume, and surface elevation is determined at the location of each centroid. Higher resolution DEMs are needed at close ranges where the sample volumes are smaller, and in areas where the radar beam grazes the surface.
- 5) Obstacles other than terrain – It is clear that towers (obstacles to navigation), buildings, and vegetation are also factors causing radar beam occultation.

A goal of the GIS-based method is to estimate the actual radar coverage of the existing and proposed radar networks. Once the individual occultation coverage grids have been determined for several adjacent radars, the *mosaic* method can then be used to assemble a radar coverage grid for an entire region. Figure 12 shows the

mosaic of five radars over North-Central Colorado, including the Front Range (Cheyenne, WY (KCYS), Denver/Boulder, CO (KFTG), and Pueblo, CO (KPUX)), Grand Mesa, CO (KGJW), and Riverton, WY (KRIW). A regional floor is found by combining all radar grids for the parameter "FLOOR" with the MINIMUM analysis condition, and after application of the *setnull* method, so that only detectable areas of the atmosphere are combined. The key conclusion is that full radar capabilities are realized in the immediate vicinity of each radar, but may be limited to higher altitudes in remote areas due to both distance to a radar as well as occultation by terrain. In some regions between KGJW and KRIW, the radar floor appears to be as much as 4000 m above ground level. This analysis approach clearly identifies localities which may be at risk for poor detection of low-altitude weather, due to the characteristics of existing or planned radar coverage. In such areas, alternate means for weather detection must be (and are usually) employed.

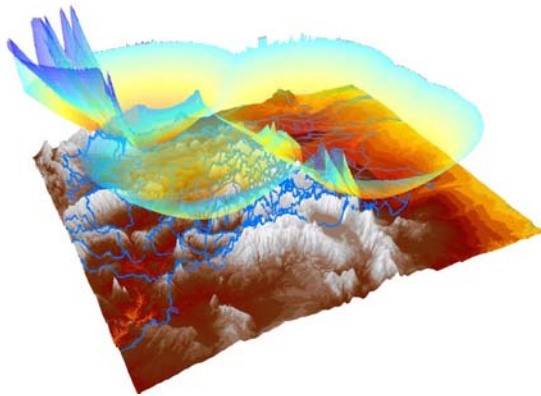


Figure 12 – Mosaic of the parameter [Floor] for five radars over North-Central Colorado, including the Front Range {Cheyenne, WY (KCYS), Denver/Boulder, CO (KFTG), and Pueblo, CO (KPUX)}, Grand Mesa, CO (KGJW), and Riverton, WY (KRIW). A regional floor is found by combining all radar grids with the MINIMUM analysis condition, and after application of the *setnull* method, so that only detectable areas of the atmosphere are combined.

5. Acknowledgments

Funding for this effort was provided by the National Weather Service under contract 50-CMAA-9-00059. The NEX2SHP utility is freeware provided courtesy of Scott T. Shipley and George Mason University. We also wish to recognize Roger Shriver, NWS retired, for his leadership in introducing GIS to NWS operations.

6. References

Ansari, S., and S. Del Greco, 2005: GIS Tools for Visualization and Analysis of NEXRAD Radar (WSR-88D) Archived at the National Climatic Data Center, Paper J9.6, 21st IIPS, AMS Annual Meeting, San Diego, CA.

http://ams.confex.com/ams/Annual2005/techprogram/paper_84729.htm

Graffman, I.A., 2004: AWIPS Map Database Home, <http://www.nws.noaa.gov/geodata/>

Leone, D.A., R.M. Endlich, J. Petročeks, R.T.H. Collis and J.R. Porter, 1989: Meteorological Considerations Used in Planning the NEXRAD Network. *Bull. Amer. Meteor. Soc.*, **70**, 4-13.

[http://ams.allenpress.com/pdfserv/10.1175/1520-0477\(1989\)070<0004:MCUIPT>2.0.CO;2](http://ams.allenpress.com/pdfserv/10.1175/1520-0477(1989)070<0004:MCUIPT>2.0.CO;2)

Saffle, R.E., R.S. Shriver and S.T. Shipley, 2003: NEXRAD to Shapefile Conversion and GIS Beam Propagation Analysis in 3D. Paper P1.23, 19th IIPS, AMS Annual Meeting, Long Beach, CA.

http://ams.confex.com/ams/annual2003/techprogram/paper_57902.htm

Shipley, S.T., Graffman, I.A., and R.E. Saffle, 2005a: Weather Radar Terrain Occultation Modeling using GIS, Paper J9.5, 21st IIPS, AMS Annual Meeting, San Diego, CA.

http://ams.confex.com/ams/Annual2005/techprogram/paper_87245.htm

Shipley, S.T., 2005b: NEX2SHP.exe version 8c utility and open source courtesy of George Mason University, Department of Geography.

<http://geog.gmu.edu/projects/wxproject/>